

## Supporting Information

### **Energy-Saving Hydrogen Production by Methanol Oxidation Reaction Coupled Hydrogen Evolution Reaction Co-Catalyzed by Phase Separation Induced Heterostructure**

Xiang Peng,<sup>a, b</sup> Song Xie,<sup>a</sup> Xia Wang,<sup>a</sup> Chaoran Pi,<sup>c</sup> Zhitian Liu,<sup>\*a</sup> Biao Gao,<sup>\*b, c</sup>

Liangsheng Hu,<sup>d</sup> Wei Xiao,<sup>e</sup> and Paul K. Chu<sup>\*b</sup>

<sup>a</sup> Hubei Key Laboratory of Plasma Chemistry and Advanced Materials, Hubei Engineering Technology Research Center of Optoelectronic and New Energy Materials, Wuhan Institute of Technology, Wuhan, 430205, China

<sup>b</sup> Department of Physics, Department of Materials Science and Engineering, and Department of Biomedical Engineering, City University of Hong Kong, Tat Chee Avenue, Kowloon, Hong Kong, China

<sup>c</sup> State Key Laboratory of Refractories and Metallurgy and Institute of Advanced Materials and Nanotechnology, Wuhan University of Science and Technology, Wuhan, 430081, China

<sup>d</sup> Department of Chemistry and Key Laboratory for Preparation and Application of Ordered Structural Materials of Guangdong Province, Shantou University, Shantou, Guangdong, 515063, China

<sup>e</sup> School of Resource and Environmental Sciences, Hubei International Scientific and

Technological Cooperation Base of Sustainable Resource and Energy, Wuhan  
University, Wuhan, 430072, China

\*Correspondence: [able.ztliu@wit.edu.cn](mailto:able.ztliu@wit.edu.cn) (Z. Liu); [gaobiao@wust.edu.cn](mailto:gaobiao@wust.edu.cn) (B. Gao);  
[paul.chu@cityu.edu.hk](mailto:paul.chu@cityu.edu.hk) (Paul K. Chu)

## (1) Preparation of mono-metal-based selenides

NiSe/CC was fabricated by a standard hydrothermal method. Ni(CH<sub>3</sub>COO)<sub>2</sub>·4H<sub>2</sub>O (0.875 mmol) and Na<sub>2</sub>SeO<sub>3</sub> (0.875 mmol) were added to a solution (35 mL) including DETA (5 mL), N<sub>2</sub>H<sub>4</sub>·H<sub>2</sub>O (10 mL), and DW (20 mL). After stirring for 30 min, the clean CC was immersed in the solution and heated to 180 °C for 12 h in an autoclave.

MoSe<sub>2</sub>/CC was prepared in two steps. 4 mmol (NH<sub>4</sub>)<sub>2</sub>MoO<sub>4</sub> and cleaned CC were added to 10 mL of DW and heated in a water bath to 70 °C. 40 mL HNO<sub>3</sub> were added dropwise and stirred in a water bath for 60 min to obtain MoO<sub>3</sub> covered CC. MoSe<sub>2</sub> on CC was prepared by a selenation process similar to the preparation of NMS/CC.

## (2) Calculation of the turnover frequency (TOF)

Calculation of TOF follows previous works <sup>1</sup>. The turnover frequency for MOR is calculated by Equation S1:

$$TOF = \frac{\text{No. of total CHOOH turnover/cm}^2 \text{ of geometric area}}{\text{No. of active sites/cm}^2 \text{ of geometric area}}$$

(Equation S1)

The total number of CHOOH turnovers per current density is calculated by Equation S2:

No. of CHOOH =

$$\left( \frac{\text{mA}}{\text{cm}^2} \right) \left( \frac{1 \text{ C s}^{-1}}{1000 \text{ mA}} \right) \left( \frac{1 \text{ mol of } e}{96485.3 \text{ C}} \right) \left( \frac{1 \text{ mol of CHOOH}}{4 \text{ mol of } e} \right) \left( \frac{6.022 \times 10^{23} \text{ CHOOH molecules}}{1 \text{ mol of CHOOH}} \right)$$

$$= 1.56 \times 10^{15} \frac{CHOOH s^{-1}}{cm^2} \text{ per } \frac{mA}{cm^2} \quad (\text{Equation S2})$$

Using the assumption that either Ni, Mo, or Se acts as the active site, the active sites per real surface can be calculated approximatively as follows:

$$\text{Active sites per ECSA}_{NiSe} = \left( \frac{2 \text{ atoms/unit cell}}{61.8 \text{ \AA}^3/\text{unit cell}} \right)^{\frac{2}{3}} = 1.016 \times 10^{15} \text{ atoms cm}_{ECSA}^{-2}$$

(Equation S3)

$$\text{Active sites per ECSA}_{MoSe_2} = \left( \frac{3 \text{ atoms/unit cell}}{121.1 \text{ \AA}^3/\text{unit cell}} \right)^{\frac{2}{3}} = 8.498 \times 10^{14} \text{ atoms cm}_{ECSA}^{-2}$$

(Equation S4)

$$\text{Active sites per ECSA}_{NMS} = \left( \frac{5 \text{ atoms/unit cell}}{182.9 \text{ \AA}^3/\text{unit cell}} \right)^{\frac{2}{3}} = 9.075 \times 10^{14} \text{ atoms cm}_{ECSA}^{-2}$$

(Equation S5)

Finally, the plot of current density is converted into a TOF plot according to the equations as follows:

$$\text{TOF} = \frac{(1.56 \times 10^{15} \frac{CHOOH s^{-1}}{cm^{-2}} \text{ per } \frac{mA}{cm^2}) \times |j|}{(\text{active sites per real surface area}) \times ECSA} . \quad (\text{Equation S6})$$

The turnover frequency for HER can also be calculated. The total number of hydrogen turnovers per current density is calculated by Equation S7:

$$\text{No. of } H_2 = \left( \text{per } \frac{mA}{cm^2} \right) \left( \frac{1 C s^{-1}}{1000 mA} \right) \left( \frac{1 \text{ mol of } e}{96485.3 C} \right) \left( \frac{1 \text{ mol of } H_2}{2 \text{ mol of } e} \right) \left( \frac{6.022 \times 10^{23} H_2 \text{ molecules}}{1 \text{ mol of } H_2} \right)$$

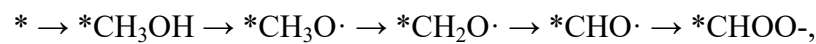
$$= 3.12 \times 10^{15} \frac{H_2 s^{-1}}{cm^2} \text{ per } \frac{mA}{cm^2} . \quad (\text{Equation S7})$$

Using the assumption that Ni, Mo, or Se acts as the active site, the active sites per real surface can be calculated approximatively by Equation S3-5. Finally, the current density plot is converted into a TOF plot according to the following equation:

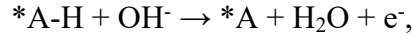
$$\text{TOF} = \frac{(3.12 \times 10^{15} \frac{H_2 s^{-1}}{cm^{-2}} \text{ per } \frac{mA}{cm^2}) \times |j|}{(\text{active sites per real surface area}) \times \text{ECSA}} \quad (\text{Equation S8})$$

### (3) Density-functional theory calculation

Density-functional theory (DFT) calculation is performed using the DMol3 program implemented in Material Studio <sup>2</sup> and the slab model with a vacuum space of 15 Å along the z-direction is adopted for NiSe<sub>2</sub>. The NiSe (101) and MoSe<sub>2</sub> (002) surfaces are selected due to the strongest diffraction signal in the XRD pattern and lattice revealed by HR-TEM. The exchange-correlation functional under the generalized gradient approximation (GGA) within the Perdew-Burke-Ernzerhof (PBE) functional is implemented <sup>3</sup>. The double-numeric quality basis set with the polarization functions (DNP) is adopted and the core electrons are treated with the DFT semi-core pseudopotentials (DSPPs) <sup>4, 5</sup>. The convergence tolerance of optimal configuration for energy, force, and maximum displacement is  $1.0 \times 10^{-5}$  Ha, 0.002 Ha/Å, and 0.005 Å, respectively. Based on previous studies, the oxidation of methanol can be described as follows <sup>6</sup>:



where \* denotes the clean electrocatalyst surface. The elemental steps are shown as follows <sup>7</sup>:



where the reaction free energy changes can be expressed as:

$$\Delta G = G_{*A} + G_{H_2O} + G_{e^-} - G_{*A-H} - G_{OH^-} \quad (\text{Equation S9})$$

$$G_{OH^-} = G_{H_2O} - G_{H^+}. \quad (\text{Equation S10})$$

Therefore,

$$\Delta G = G_{*A} - G_{*A-H} + G_{H^+} + G_{e^-}. \quad (\text{Equation S11})$$

For the calculation of  $G_{H^+} + G_{e^-}$  under the normal conditions, the computational hydrogen electrode model provided by Nørskov<sup>8</sup> is adopted to calculate the chemical potential of  $H^+ + e^-$

$$G_{H^+} + G_{e^-} = 1/2 G_{H_2}. \quad (\text{Equation S12})$$

The reaction free energy correction is calculated according to the following equation<sup>7</sup>:

$$\Delta G = \Delta E + \Delta ZPE + \Delta H - T\Delta S, \quad (\text{Equation S13})$$

where  $\Delta E$ ,  $\Delta ZPE$ ,  $\Delta H$ , and  $\Delta S$  refer to the reaction energy from the DFT calculations, the change of zero-point energy, the integrated heat capacity from 0K to 298.15 K, and the entropy change, respectively. The adsorption energy ( $E_{\text{ads}}$ ) of  $CH_3OH$  and intermediates (int.) on the surface of the substrate is defined as:

$$E_{\text{ads}} = E_{*int.} - (E_* + E_{int.}), \quad (\text{Equation S14})$$

where  $*int.$  and  $*$  denote adsorbed intermediates on the sample and bare substrate and  $E_{int.}$  denotes the energy of individual intermediates <sup>9</sup>.

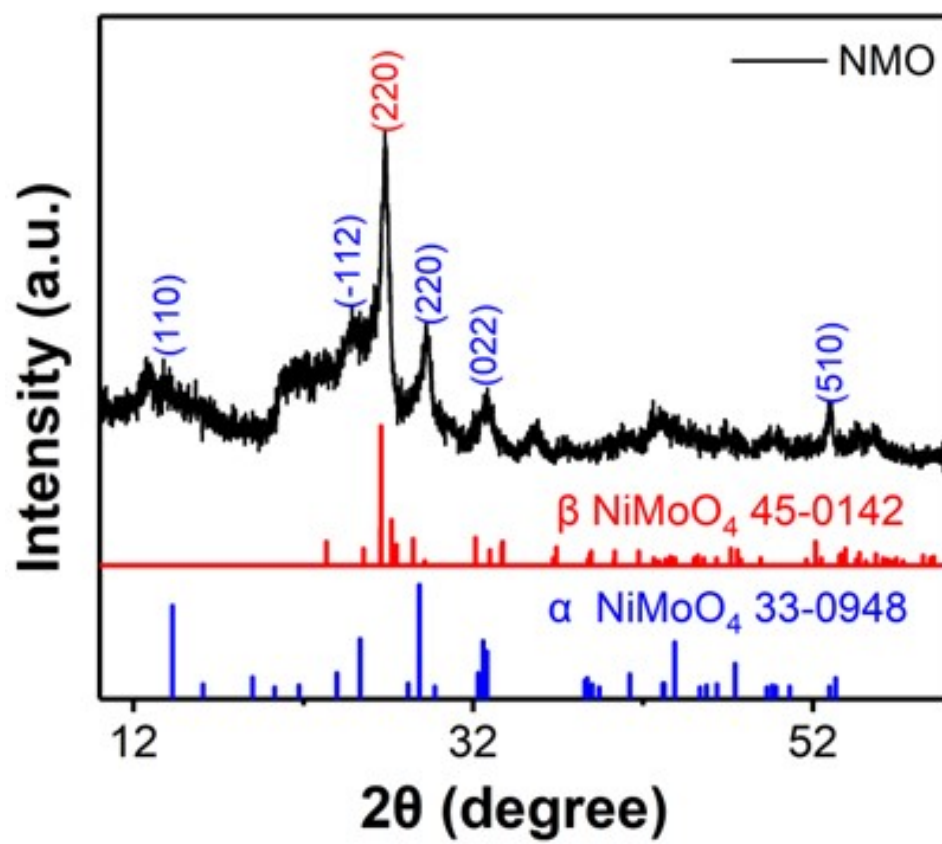


**Figure S1.** XRD spectra of NMO/CC.

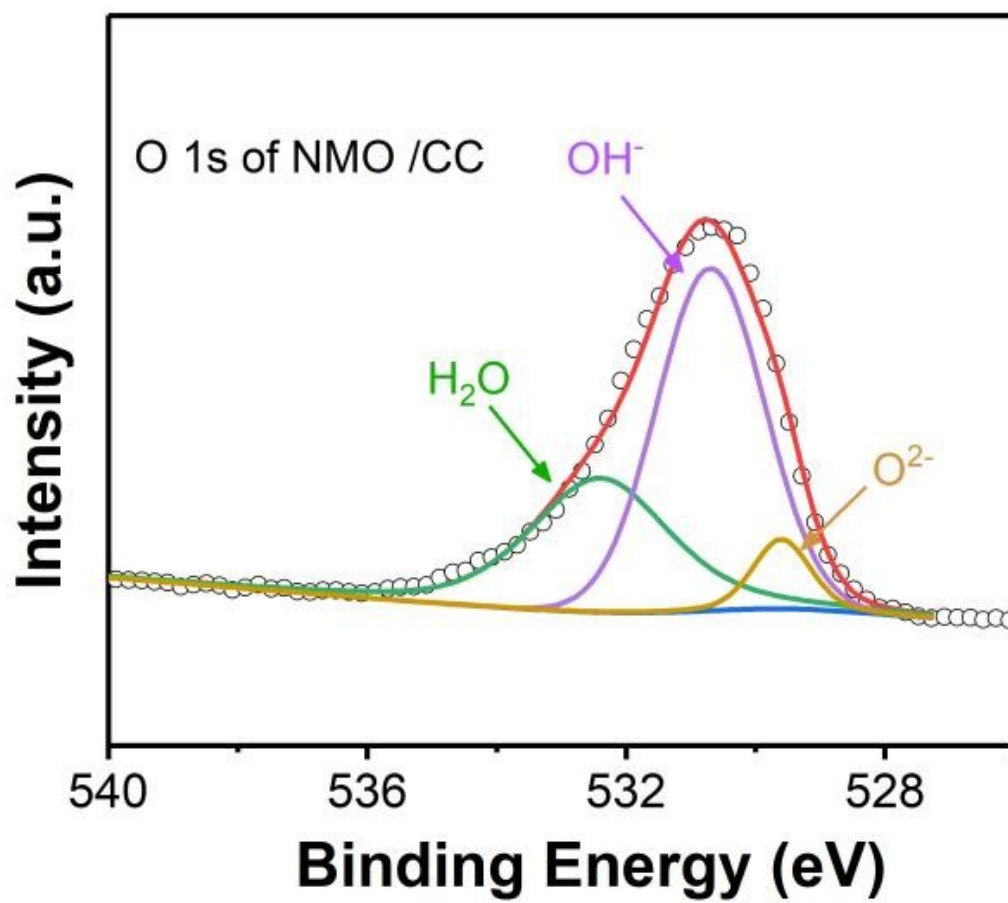


**Figure S2.** XPS of O 1s of NMO/CC catalyst.



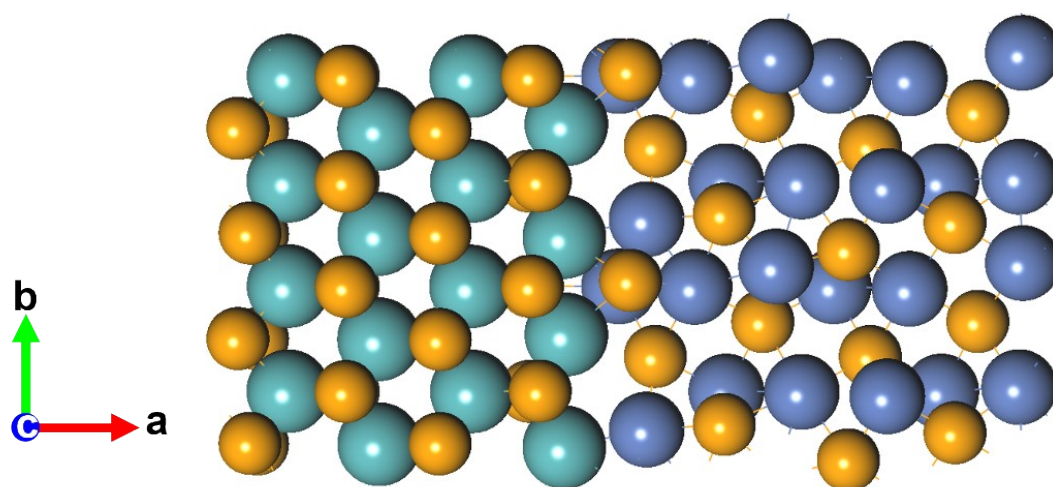


**Figure S3.** Optimized model of the surface of the MoSe<sub>2</sub>/NiSe heterostructure: Left, MoSe<sub>2</sub> (002); Right, NiSe (101).

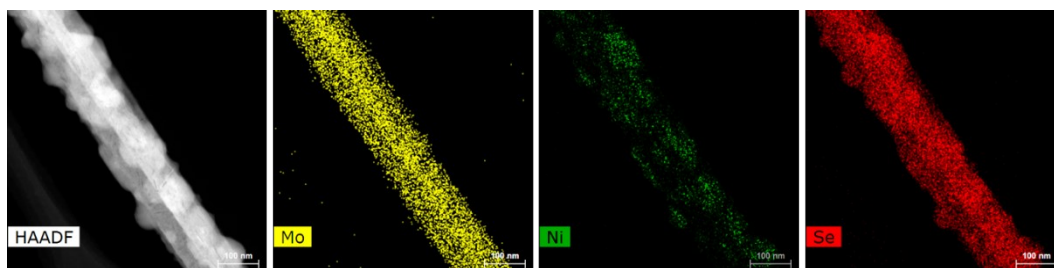


**Figure S4.** Elemental maps of tMo, Ni, and Se of the NMS nanowire.

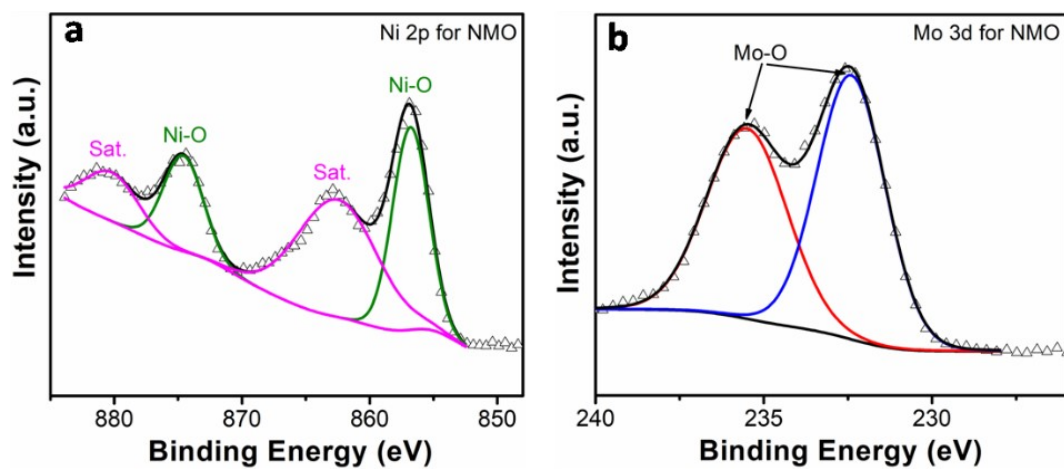


**Figure S5.** High-resolution XPS spectra of NMO/CC: (a) Ni 2*p* and (b) Mo 3*d*.

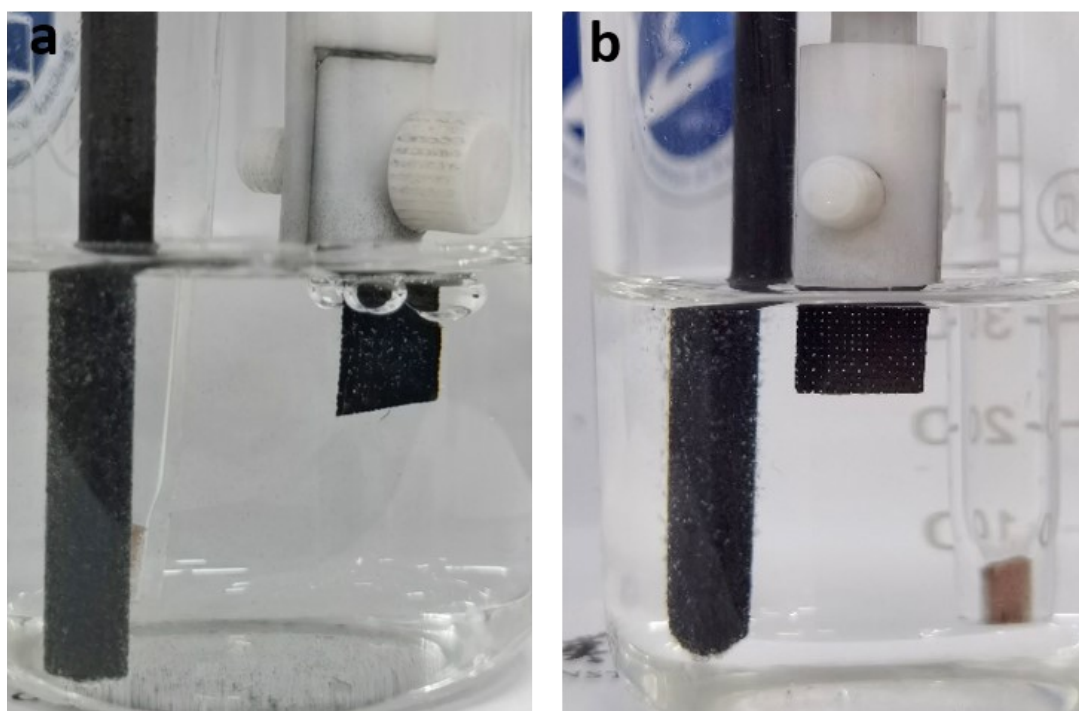


**Figure S6.** Photograph of the electrode during (a) OER and (b) MOR.

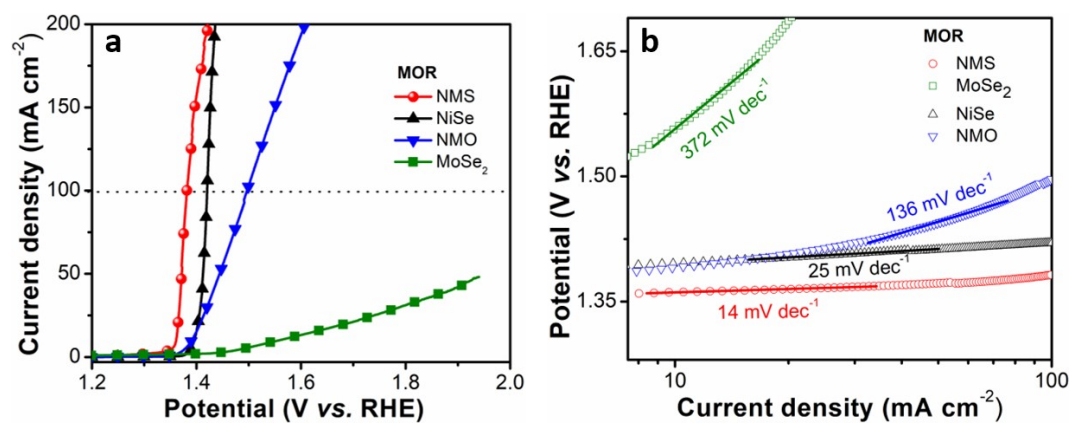


**Figure S7.** (a) Polarization curves and (b) Tafel plots of NMS/CC, NiSe/CC, NMO/CC,  $\text{MoSe}_2$ /CC for MOR.

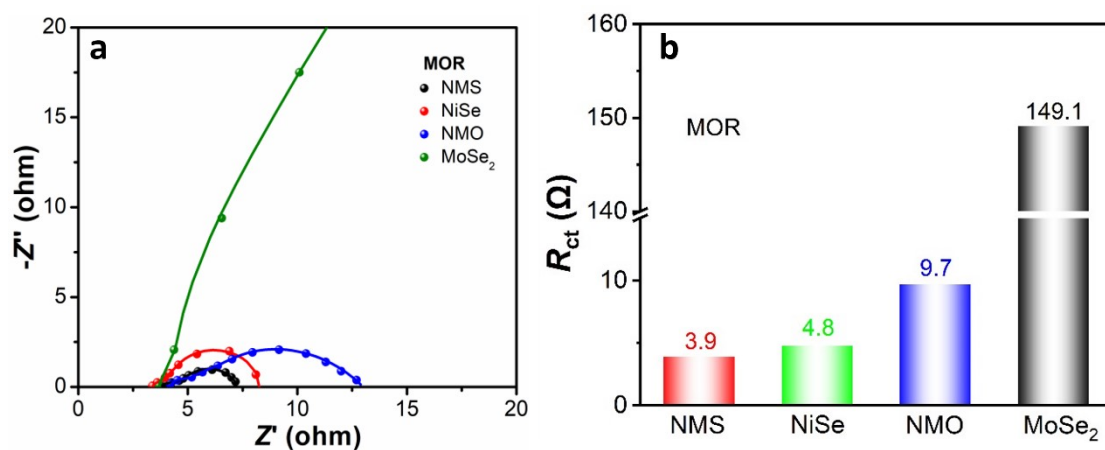


**Figure S8.** (a) EIS spectra of the NMS/CC, NiSe/CC, NMO/CC, and MoSe<sub>2</sub>/CC electrocatalysts for MOR; (b) Electron transfer resistance ( $R_{ct}$ ) of NMS, NiSe, NMO, and MoSe<sub>2</sub>.

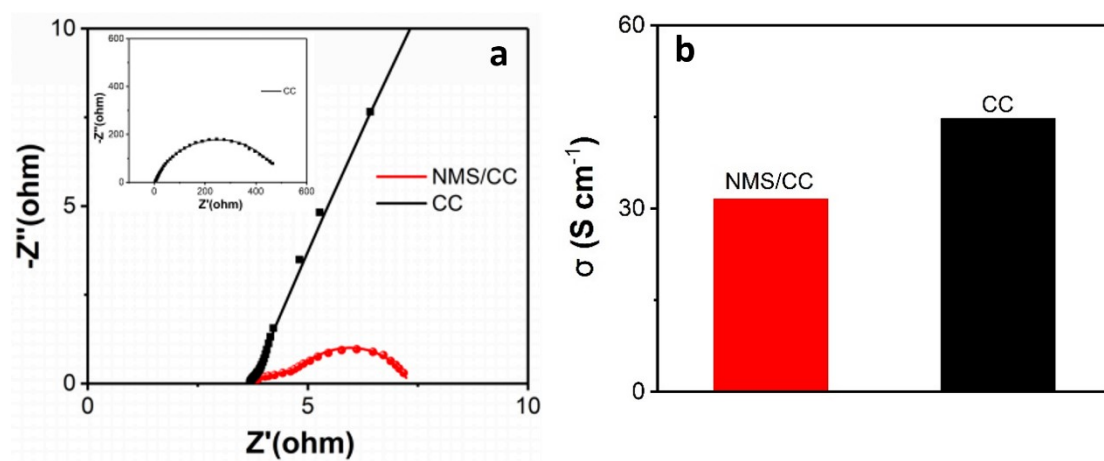


**Figure S9.** (a) EIS and (b) Electrical conductivity of the MSM/CC and CC skeleton.

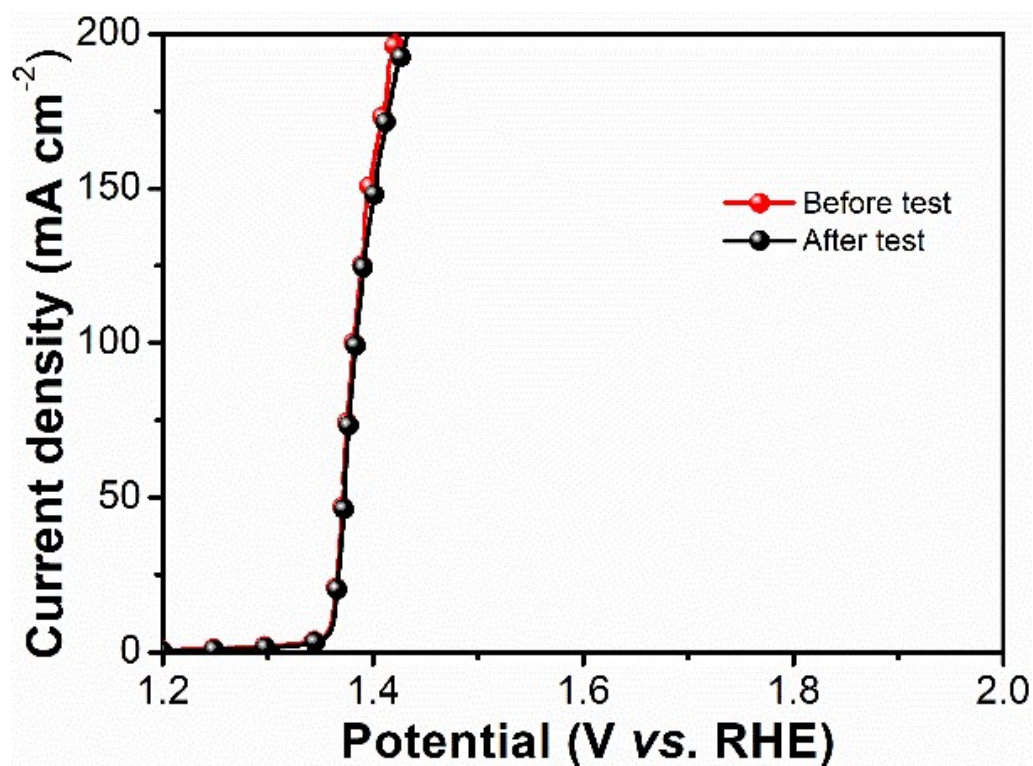


**Figure S10.** LSV curves of the NMS/CC electrocatalyst: (a) Before and (b) After the long-term continuous measurement.



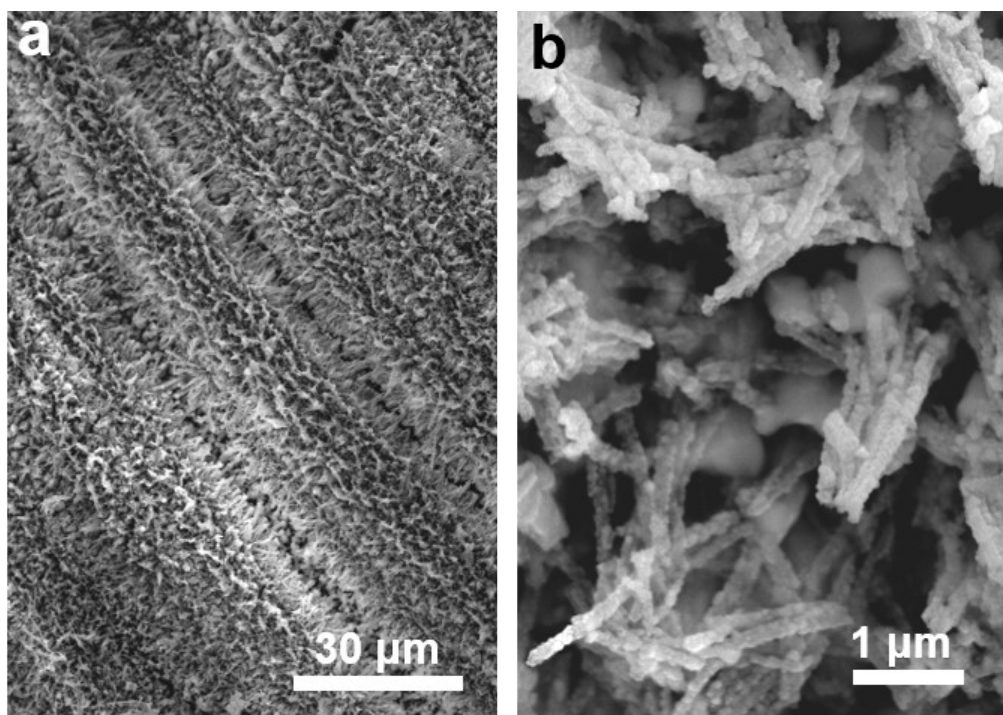


**Figure S11.** SEM images of the NMS/CC electrocatalyst after the long-term test.

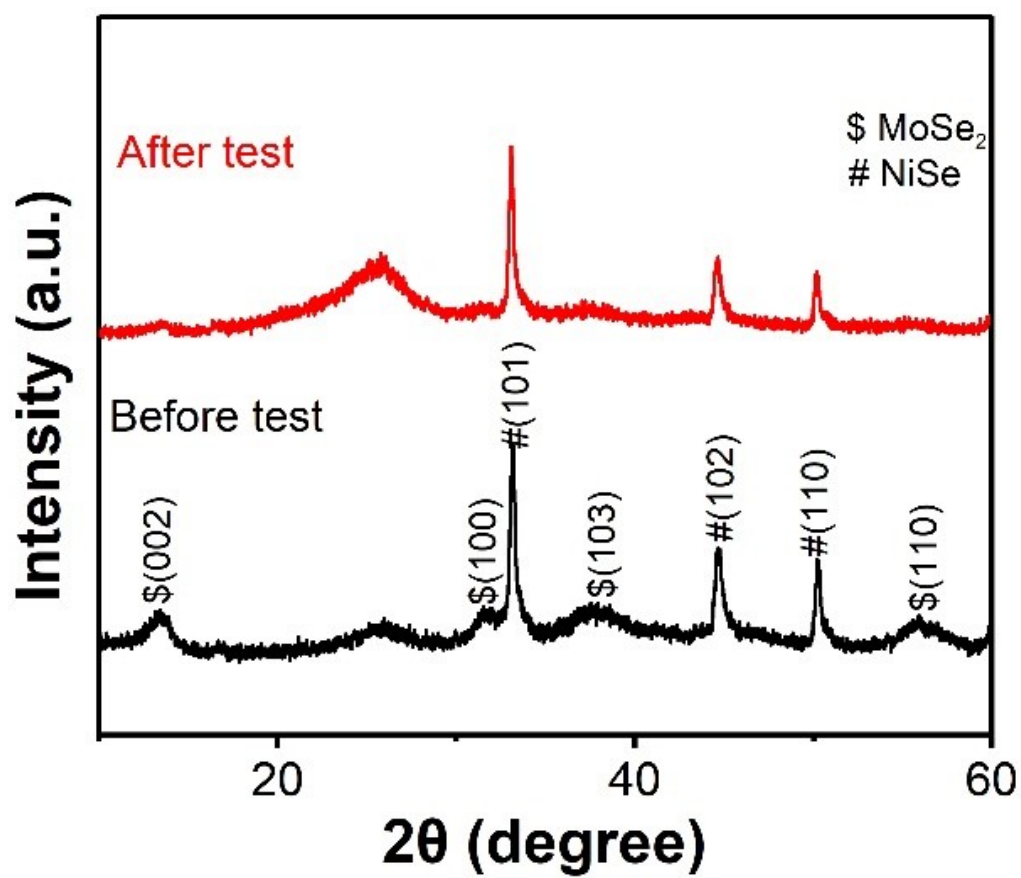


**Figure S12.** XRD spectra of the NMS/CC electrocatalyst before and after the long-term test.

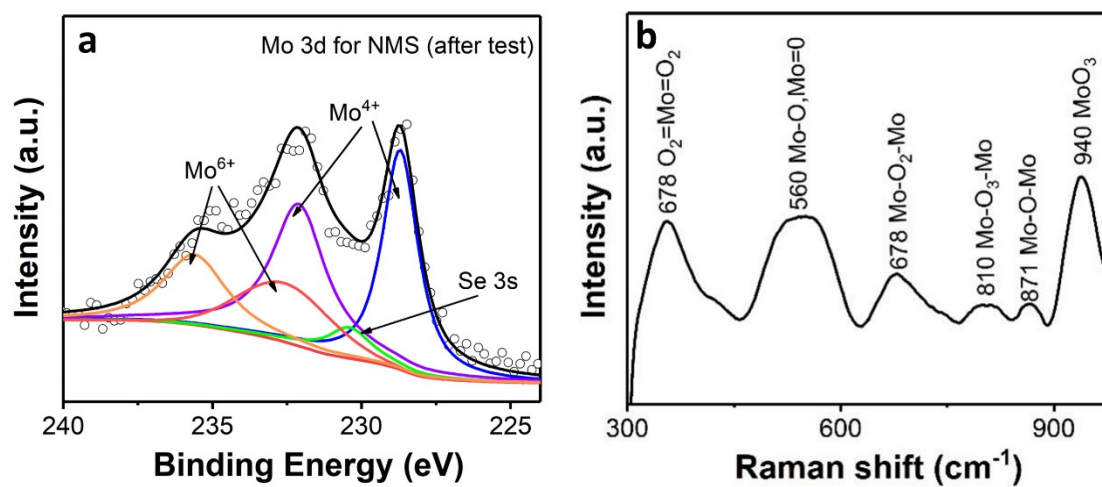


**Figure S13.** (a) XPS Mo 3d spectrum and (b) Raman spectrum of NMS/CC after the electrochemical measurement.

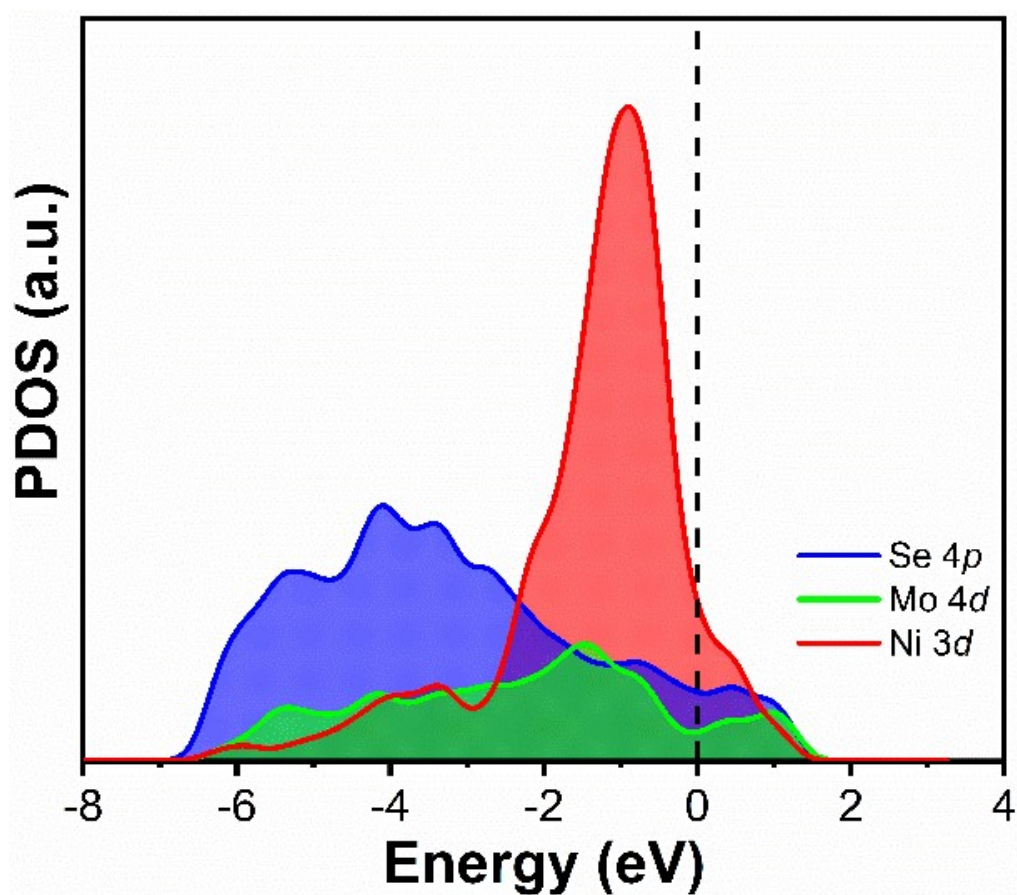


**Figure S14.** Partial density of states of Ni-3*d*, Mo-4*d*, and Se-4*p* in the NMS heterostructure.

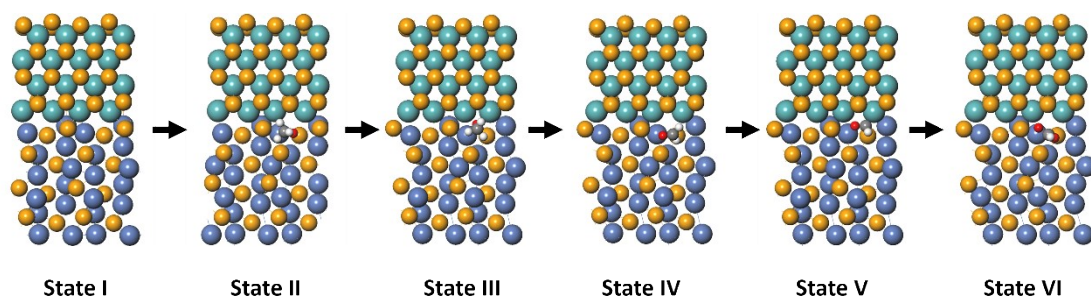


**Figure S15.** Simulated schematic diagram of the corresponding catalyst in MOR.

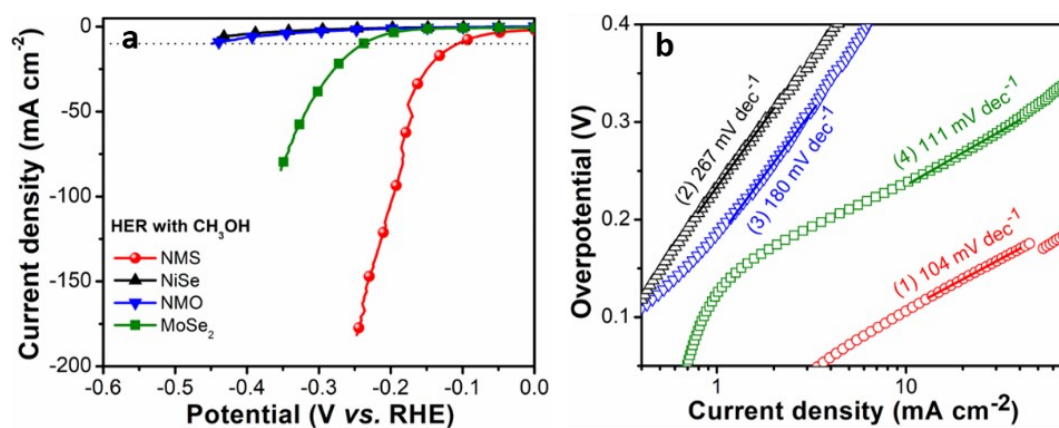


**Figure S16.** HER characteristics in 1.0 M KOH and 1.0 M  $\text{CH}_3\text{OH}$  electrolytes: (a) Polarization curves and (b) Tafel plots (1 - NMS/CC, 2 - NiSe/CC, 3 - NMO/CC, and 4 -  $\text{MoSe}_2$ /CC).

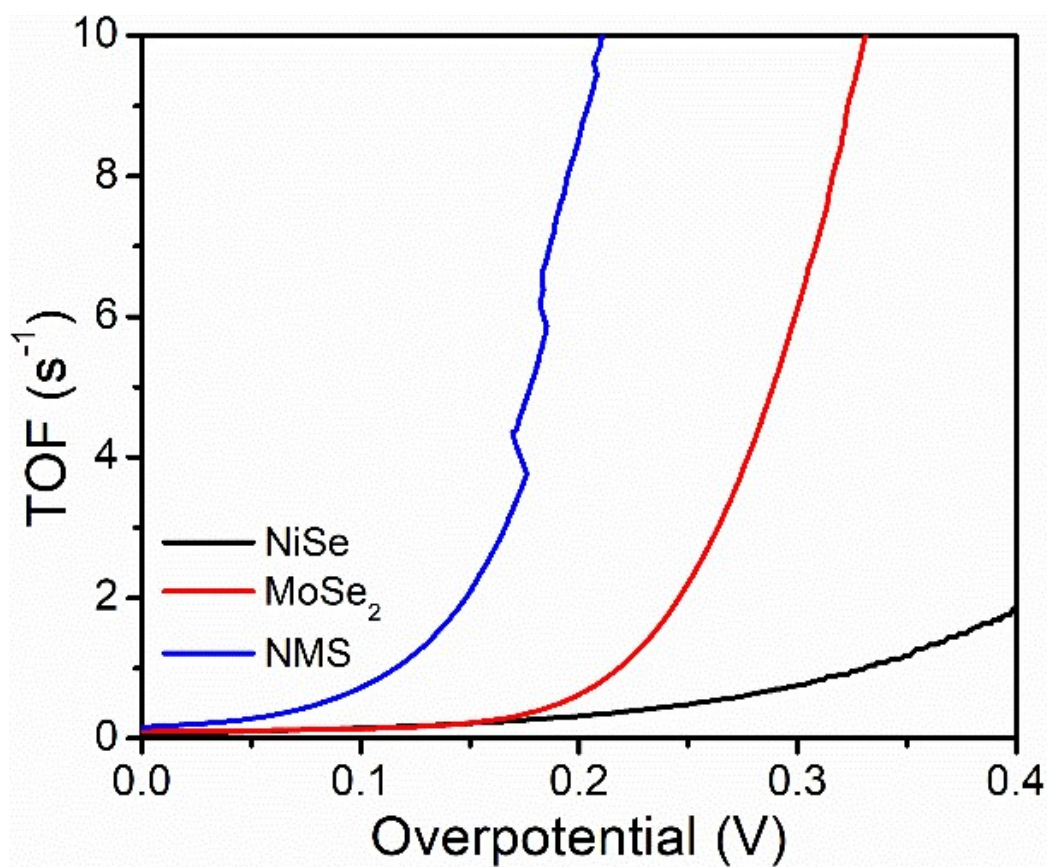


**Figure S17.** TOF plots with respect to the overpotentials of the NiSe/CC,  $\text{MoSe}_2$ /CC, and NMS/CC electrocatalysts for HER.



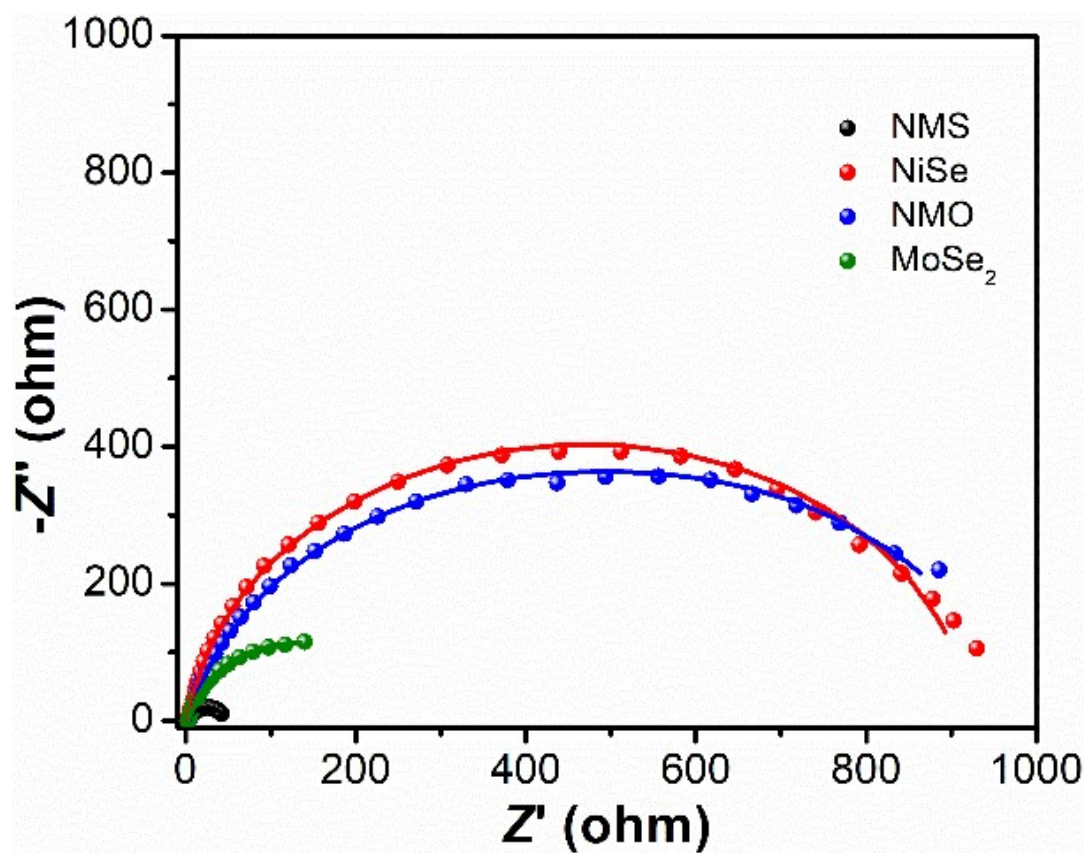


**Figure S18.** EIS plots of the electrocatalysts in HER.



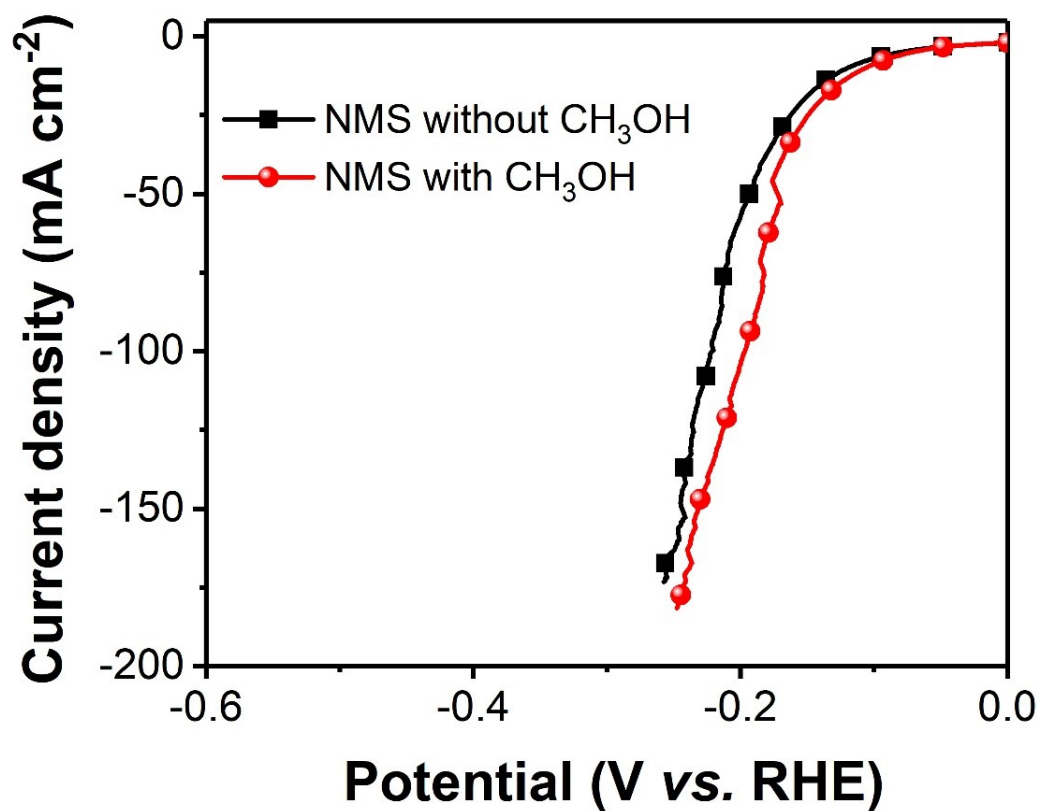


**Figure S19.** Polarization curves of the NMS/CC electrocatalyst in different electrolytes.

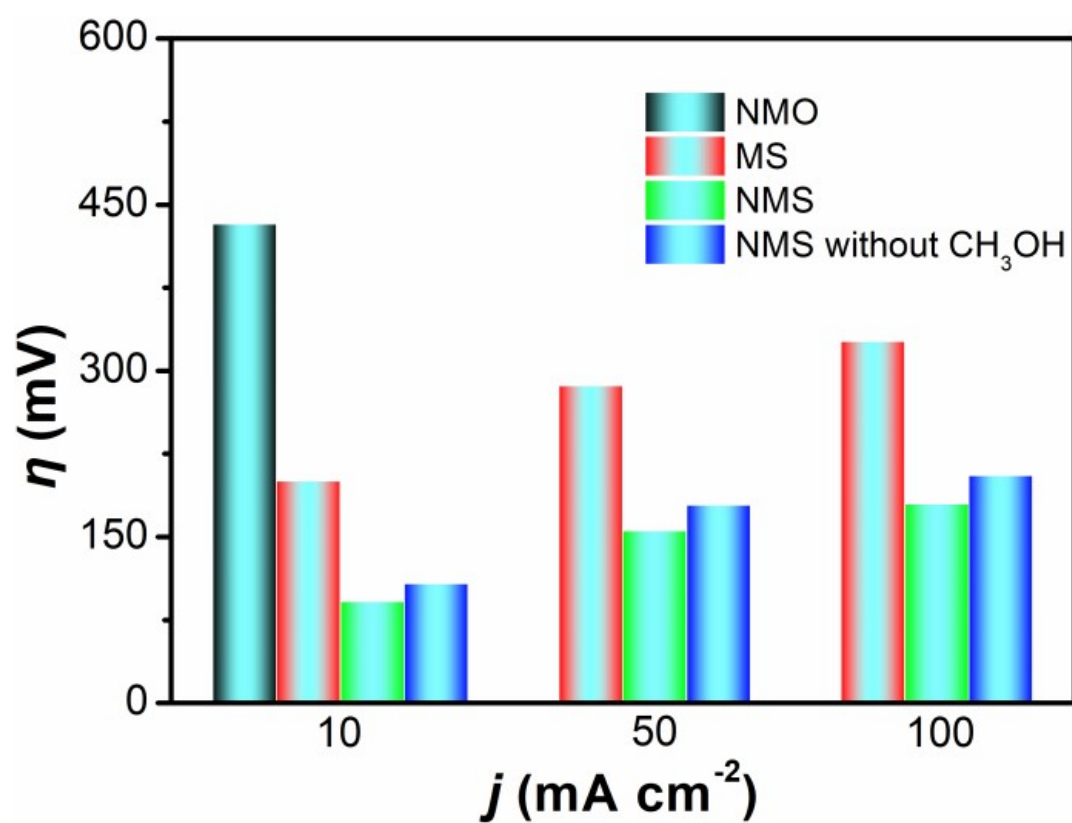


**Figure S20.** Comparison of the overpotentials at different current densities of the NMS/CC, MoSe<sub>2</sub>/CC, and NMO/CC electrocatalysts.

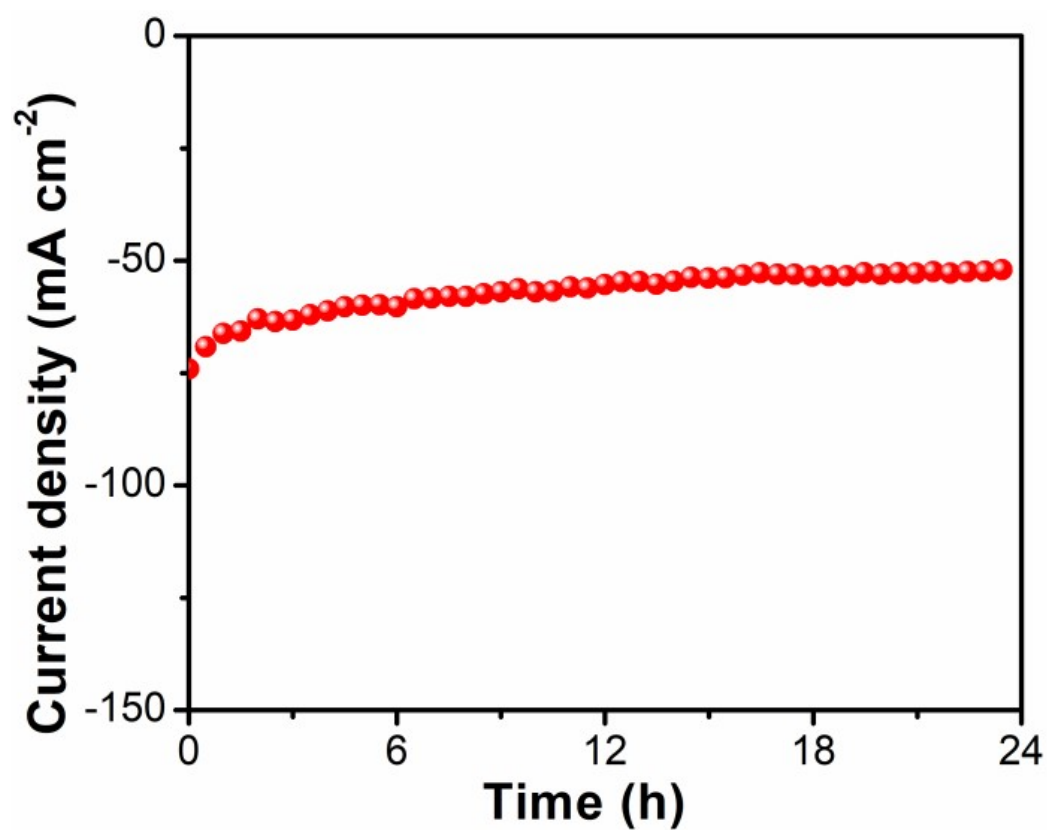


**Figure S21.** Stability of the NMS/CC electrocatalyst in HER in 1.0 M KOH and 1.0 M CH<sub>3</sub>OH.

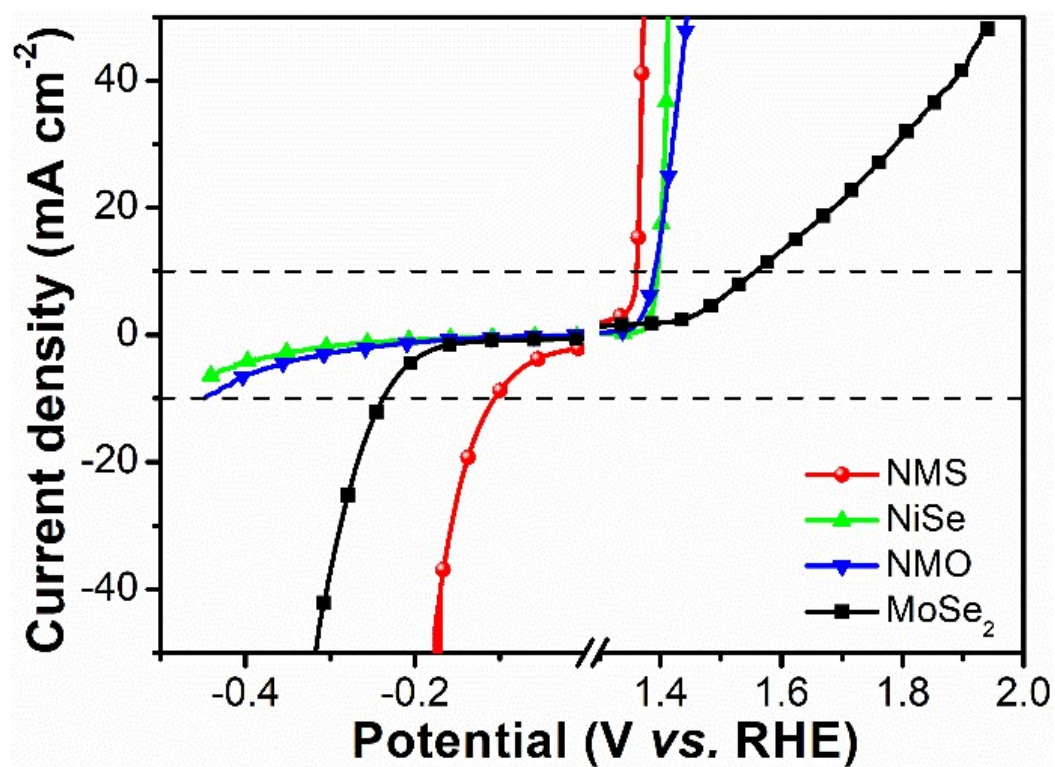


**Figure S22.** MOR and HER curves of the NMS/CC, NiSe/CC, NMO/CC, and MoSe<sub>2</sub>/CC electrocatalysts.

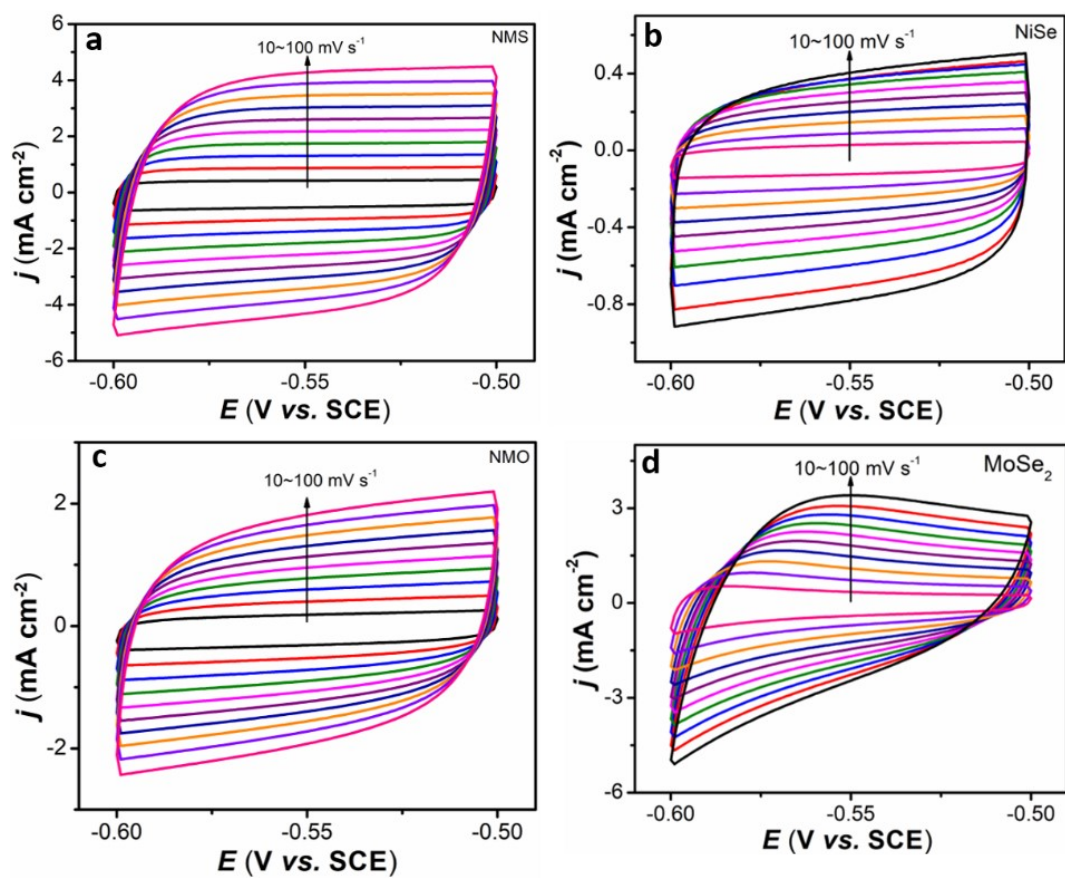


**Figure S23.** Cyclic voltammetry (CV) curves of (a) NMS, (b) NiSe, (c) NMO, and (d) MoSe<sub>2</sub> at scanning rates between 10 and 100 mV s<sup>-1</sup>.

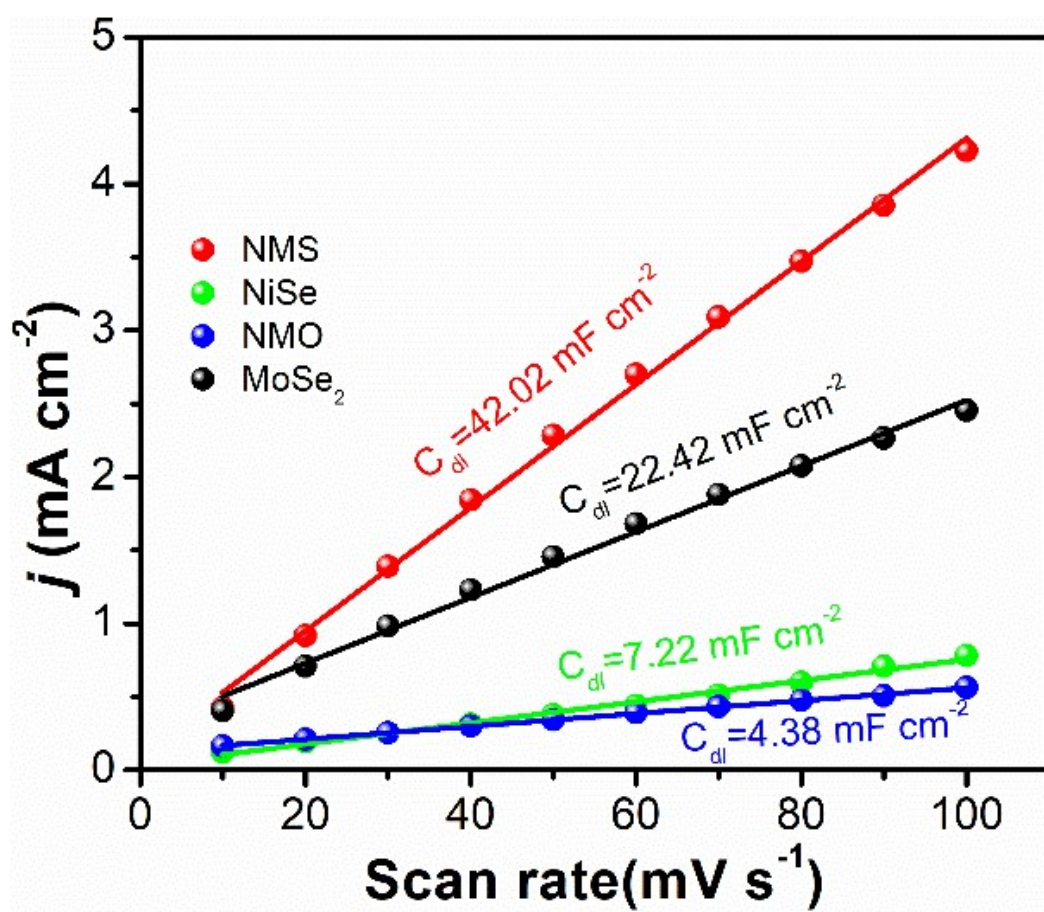


**Figure S24.** ECSA of the NMS/CC, NiSe/CC, NMO/CC, MoSe<sub>2</sub>/CC electrocatalysts.

## References

- 1 Y. Luo, Y. Wu, D. Wu, C. Huang, D. Xiao, H. Chen, S. Zheng and P. K. Chu, *ACS Appl. Mater. Interfaces*, 2020, **12**, 42850-42858.
- 2 B. Delley, *The Journal of Chemical Physics*, 1990, **92**, 508-517.
- 3 J. P. Perdew, K. Burke and M. Ernzerhof, *Phys. Rev. Lett.*, 1996, **77**, 3865-3868.
- 4 S. Grimme, *J. Comput. Chem.* , 2004, **25**, 1463-1473.
- 5 S. Grimme, *J. Comput. Chem.* , 2006, **27**, 1787-1799.
- 6 Q. Ding, W. Xu, P. Sang, J. Xu, L. Zhao, X. He and W. Guo, *Appl. Surf. Sci.*, 2016, **369**, 257-266.
- 7 L. Xiong, Z. Sun, X. Zhang, L. Zhao, P. Huang, X. Chen, H. Jin, H. Sun, Y. Lian, Z. Deng, M. H. Rümmerli, W. Yin, D. Zhang, S. Wang and Y. Peng, *Nat. Commun.*, 2019, **10**, 3782.
- 8 J. K. Nørskov, J. Rossmeisl, A. Logadottir, L. Lindqvist, J. R. Kitchin, T. Bligaard and H. Jónsson, *J. Phys. Chem. B*, 2004, **108**, 17886-17892.
- 9 C. Pi, Z. Zhao, X. Zhang, B. Gao, Y. Zheng, P. K. Chu, L. Yang and K. Huo, *Chem. Eng. J.*, 2021, **416**, 129130.